OAK RIDGE NATIONAL LABORATORY

operated by

UNION CARBIDE CORPORATION

NUCLEAR DIVISION

for the

U.S. ATOMIC ENERGY COMMISSION

UNION CARBIDE

ORNL - TM - 1891

COPY NO. - **125**

DATE - Aug. 24, 1967

Neutron Physics Division

NEUTRONS FROM ^{9}Be(α,n) REACTION FOR E_α BETWEEN 6 AND 10 MeV

V. V. Verbinski,* F. G. Perey, J. K. Dickens, and W. R. Burrus

ABSTRACT

Absolute differential cross sections have been measured for the reaction ^{9}Be$(\alpha,n)^{12}$C leaving ^{12}C in its ground, first-excited, and second-excited states as a function of angle and alpha bombarding energy. The angular distribution for the ground-state (0+ state) transition changed from a fore-aft peaking at $E_\alpha = 6.8$ MeV to a three-peaked angular distribution at $E_\alpha = 9.9$ MeV. Similar behavior was observed for the second-excited-state transition (0+). The angular distribution for the first-excited-state transition (2+) displayed fore-aft peaking and was not sensitive to bombarding energy. A strong, low-energy neutron component, present at forward angles at all bombarding energies, can be accounted for by three- and four-body breakup reactions. We determined that neutrons with energy ≤ 0.5 MeV account for ~ 30% of the total neutron production cross section from this reaction.

*Present address: General Atomic, San Diego, California

TABLE OF CONTENTS

I. INTRODUCTION

Energy spectra of neutrons produced by $^4\text{He}^{++}$ ion bombardment of ^9Be were measured as a function of neutron emission angle θ and bombarding energy E_α, for E_α = 6 to 10 MeV. Three neutron groups, the n_0, n_1, and n_2 neutron groups from the $^9\text{Be}(\alpha,n)^{12}\text{C}$ reaction, leaving ^{12}C in the ground, first, and second excited states, were well resolved in these spectra. Below these groups lay a continuum of lower energy neutrons from the very broad n_4 level and from other, lower Q value, reactions. Without a complex shape analysis[1] these low-energy neutron groups cannot be resolved, so that the low-resolution neutron spectrometer used for these measurements proved to be an adequate choice.

Angular distributions reported previously for E_α = 6 MeV (Ref. 2) and 10 to 22 MeV (Ref. 3,4) indicate that for the n_0 group the data are insensitive to bombarding energy E_α from 10 to 22 MeV but that at E_α = 6 MeV the angular distribution is quite different. The present measurements therefore fill in the gap for this interesting case, and for the n_1 and n_2 angular distributions as well.

The neutron spectrum above 0.5 MeV (the cutoff value for the spectrometer used) and below the n_2 group is of interest in determining the source of the abundant low-energy neutrons. These spectra have been angle-integrated to produce $\sigma(E_n)$ and the results analyzed. The $\sigma(E_n)$ for $E_n > 0.5$ MeV were then integrated over energy, and the total cross section so obtained was compared with the flat-counter measurements of Gibbons and Macklin[5] to determine the approximate spectral behavior below the 0.5-MeV cutoff of our spectrometer.

II. EXPERIMENTAL PROCEDURE

A beam of $^4\text{He}^{++}$ ions obtained from the ORNL 5-MV Van de Graaff accelerator was energy analyzed with a 90-deg bending magnet, collimated, and focused on a beryllium metal target deposited on a platinum backing. The target was located at the end of a long Faraday cup. The target thickness was ≈ 1 mg/cm^2, producing an energy spread of approximately 350 keV at 10-MeV bombarding energy.

The sensing element of the neutron spectrometer was a 5-cm-diam by 5-cm-high cylinder of NE-213* liquid organic scintillator. It was mounted on an RCA 6810A photomultiplier tube and positioned 45 cm from the beryllium target. A linear signal was obtained at dynode 10 and a pulse shape discrimination (PSD) signal obtained from a modified Forté type PSD circuit[6,7] which utilizes pulses from dynode 14 and anode. This circuit rejected gamma-ray pulses and identified proton-recoil neutron events down to about 0.3-MeV neutron energy (equivalent electron energy $\sim$ 40 keV.)

The pulses due to neutrons were sorted in a pulse-height analyzer, and the energy spectrum was obtained by unfolding the pulse-height distribution with the FERDoR code[7]. This code utilizes a response matrix[8] obtained in an extended program of calibrating the organic scintillator response to monoenergetic neutrons for a large number of neutron energies.

The spectrometer was also used to obtain the integrated neutron flux from a Po-Be neutron source calibrated by the National Bureau of Standards, and agreement with the NBS value was better than 5%. The Po-Be spectrum is shown in Fig. 1, along with some careful nuclear emulsion measurements taken from the literature.[9,10]
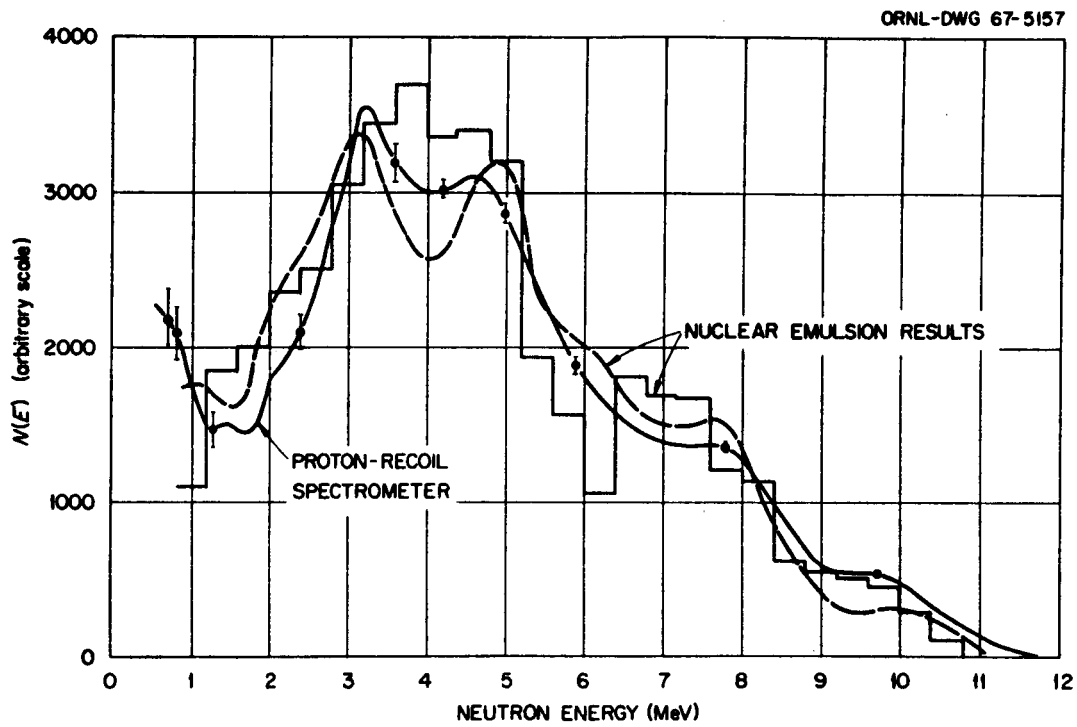
*Nuclear Enterprises Ltd., Winnipeg, Canada.

Fig. 1. Proton Recoil Spectrometer Results for Po-Be Neutron Spectrum Compared with Nuclear Emulsion Results of Ref. 9 (Dashed Curve) and Ref. 10 (Histogram). The small (~ 2 cm x 2 cm) source, calibrated at the National Bureau of Standards, was used in determining the accuracy of the spectrometer calibration (5%).

The errors assigned to the neighboring points in the output of the FERDoR unfolding code are highly correlated. Therefore, the percentage error for the area under a peak was conservatively taken as about half the percentage error of the highest point. The systematic error is estimated to be 10%. Two independent evaluations of systematic error are given in Sections III.B. and III.E. below. The sources of error include detector calibration, current integrator calibration, Faraday cup "leakage," and target thickness uncertainty.

Angular distributions were measured for target and background contributions. The background was measured with a plain platinum foil as a target, and was the order of 1^d. Carbon deposition on the beryllium target and on the plain platinum blank was kept very low by using a liquid nitrogen trap to remove diffusion-pump oil from the region of the target.

Floor scattering was ignored because only a small fraction of the source neutrons struck the floor nearby. With a 10% estimate of fast neutron albedo from concrete, a spectrometer energy cutoff of 0.5 MeV, and an R^2 advantage of 10 for source neutrons compared with concrete albedo neutrons, the estimated floor scattering component was well below 1%.

III. THE WELL RESOLVED LEVELS

A. The Energy Spectrum

In Fig. 2a is shown the pulse-height distribution at 0 deg for $E_\alpha = 7.96$ MeV, and in Fig. 2b is shown the corresponding energy spectrum reduced to $\sigma(\theta,E)$, the neutron production cross section in laboratory coordinates. The three well resolved levels corresponded to n_0, n_1, and n_2 neutron groups from the $^9Be(\alpha,n)^{12}C$ reaction, and were converted to $\sigma_0(\theta)$, $\sigma_1(\theta)$, and $\sigma_2(\theta)$ in the center-of-mass system.

ORNL-DWG 67-5158
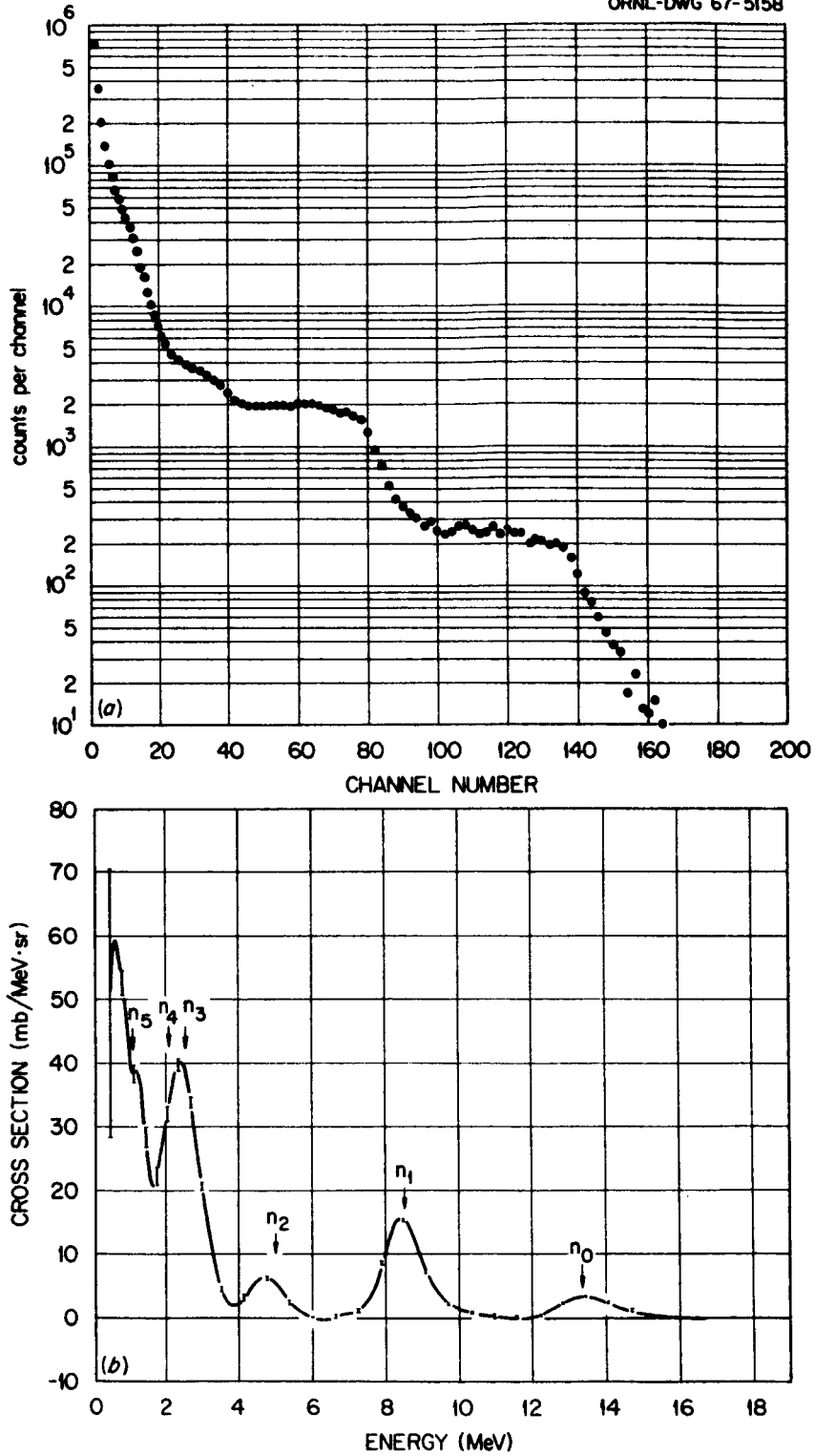

Fig. 2. Cross Section for ^{9}Be(α,n) Reactions (Lab System) at 0 deg for $\overline{E_\alpha} = 7.96$ MeV. The arrows show the energies of the neutron groups from ^{9}Be$(\alpha,n)^{12}$C, ^{12}C,* assuming narrow line width.

B. The n_0 Group

The variation of the cross section of n_0 neutrons with angle is shown in Fig. 3 for E_α = 6.79, 7.96, 8.91, and 9.92 MeV. At the three highest energies a three-peaked angular distribution is observed which does not change much with E_α. However, the angular distribution changes significantly between 7.96 and 6.79 MeV. At the lowest energy, it takes on a two-peaked shape that is very much like the fore-aft peaking reported by Gale and Garg[2] at E_α = 5.5 to 6 MeV. At the three higher energies, the angular distributions are similar to those reported by Kjellman and Nilsson[3] for E_α = 10 to 14 MeV and by Kondo et al.[4] for E_α = 17.5 to 22 MeV. Thus, $\sigma_0(\theta)$ shows little dependence on E_α between 8 and 22 MeV. Borrowing from the conclusions of Kjellman and Nilsson,[3] the constancy of angular distribution indicates that direct reaction mechanisms dominate in the $^9Be(\alpha,n_0)^{12}C$ reaction for $E_\alpha > 8$ MeV. Below 8 MeV, strong interference from the compound nucleus effect may become important, as evidenced by rapid variations of $\sigma_0(\theta)$ with E_α.

Integration of $\sigma_0(\theta)$ over angle yielded σ_0 at the four values of E_α. The results presented in Table I show a peak at 8 MeV, then a gradual decrease to E_α = 10 MeV. The value of $\sigma(\alpha,n_0)$ at 9.92 MeV is 22 ± 2 mb, and compares favorably with the value 24 ± 6 mb calculated from the observed cross section $\sigma(n,\alpha_0) = 80 \pm 20$ mb (Ref. 11) for the inverse ground state transition, $^{12}C(n,\alpha_0)^9Be$ at $E_n = 14.1$ MeV. The agreement is very good and serves as an independent check on our systematic error. In addition, we calculated the cross sections of the $^{12}C(n,\alpha)^9Be$ ground state transition for the four neutron bombarding energies corresponding to E_α = 6.79, 7.96, 8.91, and 9.92 MeV and neutron bombarding energies of 11.3, 12.1, 12.8, and 13.6 MeV (see Table I).

ORNL-DWG 67-5159
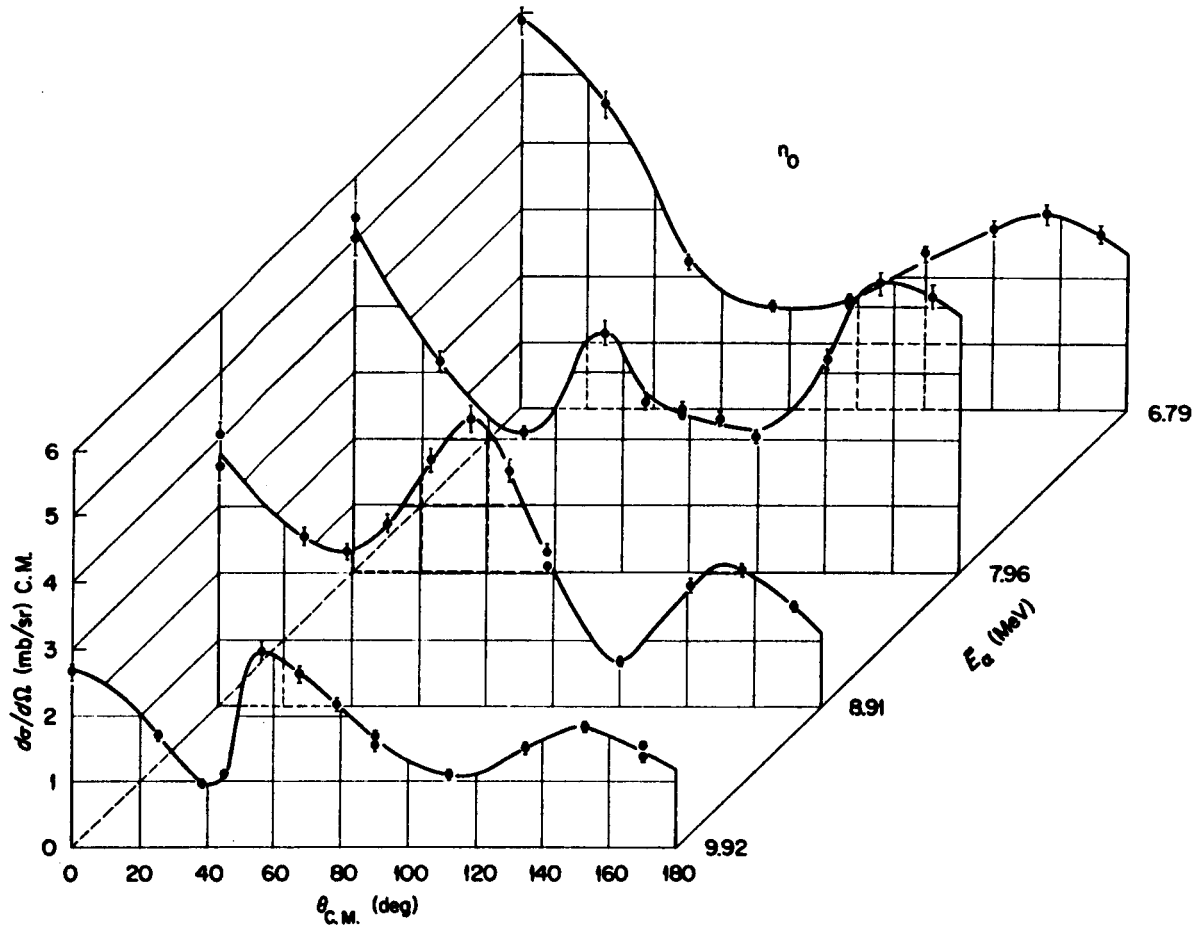
Fig. 3.   Cross Section (c.m.) Versus Angle of n_0 Neutrons for Four Values of $\overline{E}_\alpha$.

TABLE I.

Total cross section for the well separated neutron groups, n_0, n_1, and n_2. The total cross section for the inverse $^{12}C(n, \alpha_0)^9Be$ reaction and the corresponding neutron bombarding energy are shown, as calculated from the $^9Be(\alpha, n_0)$ cross section.[††]

E_α (lab) (MeV)	$\sigma(\alpha,n)$(mb)			$\sigma(n, \alpha_0)$ (mb)	E_n (lab) (MeV)
	n_0	n_1	n_2		
6.79	30	138	31	81	11.3
7.96	36	113	24	103	12.1
8.91	30	66	19	93	12.8
9.92	22	74	13	72	13.6

[††] The reciprocity relation $\sigma(n, \alpha_0)(2I_1 + 1) M_\alpha E_\alpha = \sigma(\alpha, n_0)(2I_2 + 1) M_n E_n$ was used. $I_1 = 3/2$, $I_2 = 1/2$, M_α and M_n are reduced masses, and E_α, E_n are in the center-of-mass system.

C. The n_1 Group

In Fig. 4 is shown $\sigma_1(\theta)$ for four values of E_α. The angular distributions display a persistent fore-aft peaking with a small third peak at the highest and lowest values of E_α. They are much like those reported by Kjellman and Nilsson[3] at 10 and 11 MeV, and somewhat similar to the fore-aft peaking reported by Gale and Garg[2] at E_α = 5.5 to 6 MeV. Thus, the variation of $\sigma_1(\theta)$ with E_α is rather small between 5.5 and 11 MeV. The difference in shape between $\sigma_0(\theta)$ and $\sigma_1(\theta)$ must be related to the spins and parities (0+ and 2+ respectively) of the two corresponding levels for the ^{12}C residual nucleus.

D. The n_2 Group

The variation of $\sigma_2(\theta)$ with E_α, as seen in Fig. 5, is quite pronounced. At E_α = 9.92 MeV, three peaks can be seen. This changes to a two-peaked angular distribution at E_α = 8.91 MeV, and to a strong forward-peaked shape at E_α = 7.96 and 6.79 MeV. At the lowest value of E_α, $\sigma_2(\theta)$ is very much like the three angular distributions for E_α = 5.5 to 6 MeV (Ref. 2); while for E_α = 9.92 MeV, the shape of $\sigma_2(\theta)$ is very much like that reported for E_α = 9.8 MeV (Ref. 3). Little variation of $\sigma_2(\theta)$ was observed for E_α between 10 and 14 MeV, where $\sigma_2(\theta)$ looks very much like $\sigma_0(\theta)$. This similarity must be related to the fact that both final levels in ^{12}C have J^π = 0+.

E. The 0-deg Excitation Functions

The 0-deg excitation functions are shown in Fig. 6 for the n_0, n_1, and n_2 neutron groups for E_α = 6 to 10 MeV. The n_0 excitation function is in reasonably good agreement with the high resolution (in E_α) results of Miller and Kavanagh[12] (data obtained using a stilbene crystal). However, our n_1 and n_2 curves are 50 to 80% higher; apparently the presence of the 4.43-MeV gamma-ray pulses (which they used to obtain the

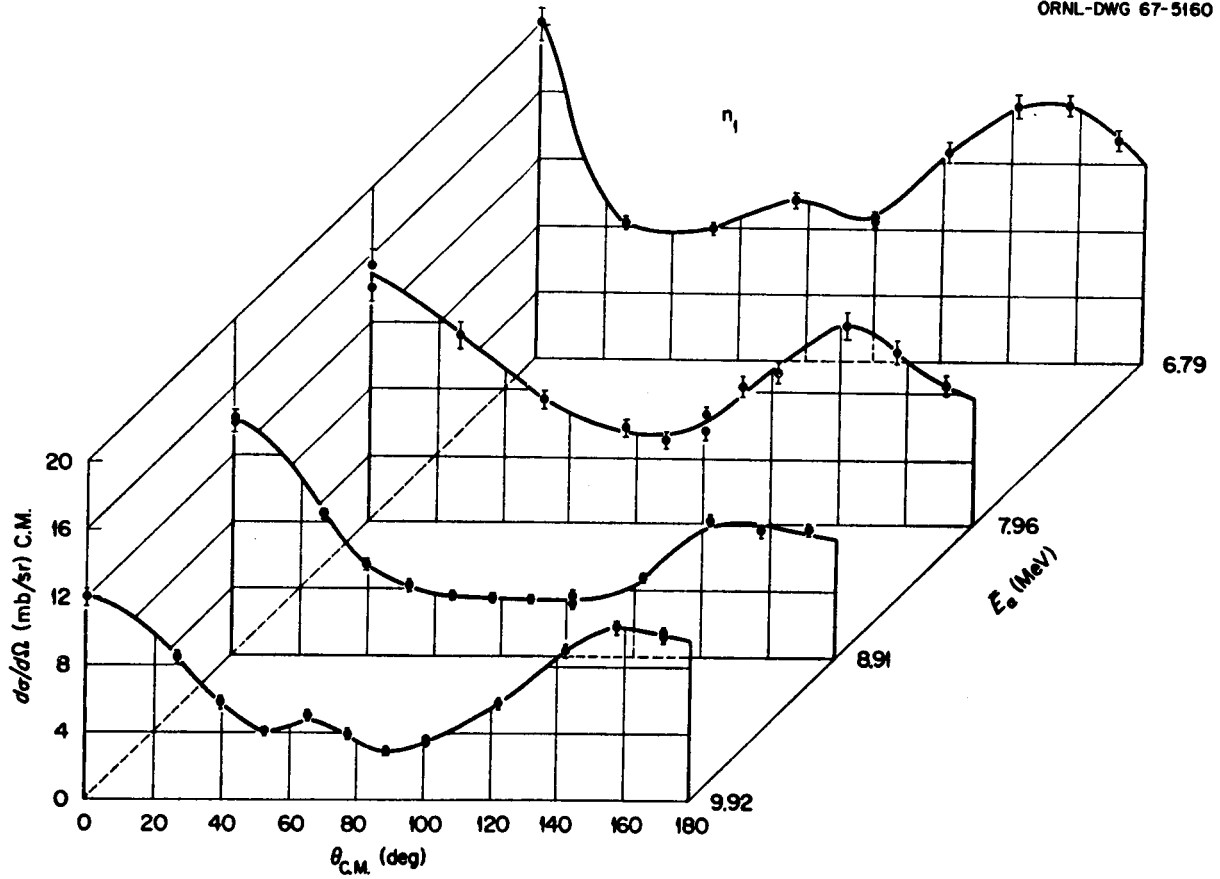Fig. 4. Cross Section (c.m.) Versus Angle of n_1 Neutrons for Four Values of $\overline{E}_\alpha$.
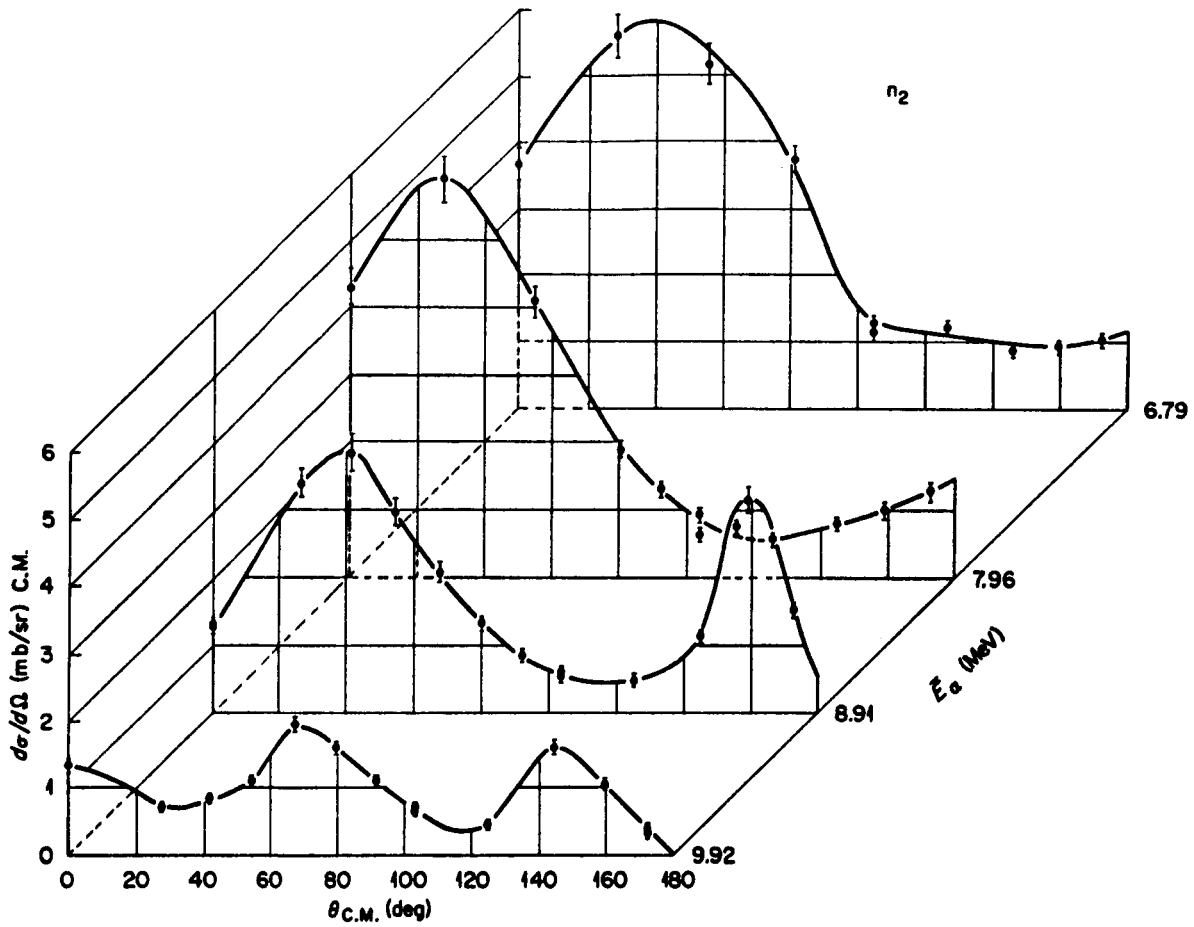
Fig. 5. Cross Section (c.m.) Versus Angle of n_2 Neutrons for Four Values of $\overline{E}_\alpha$.
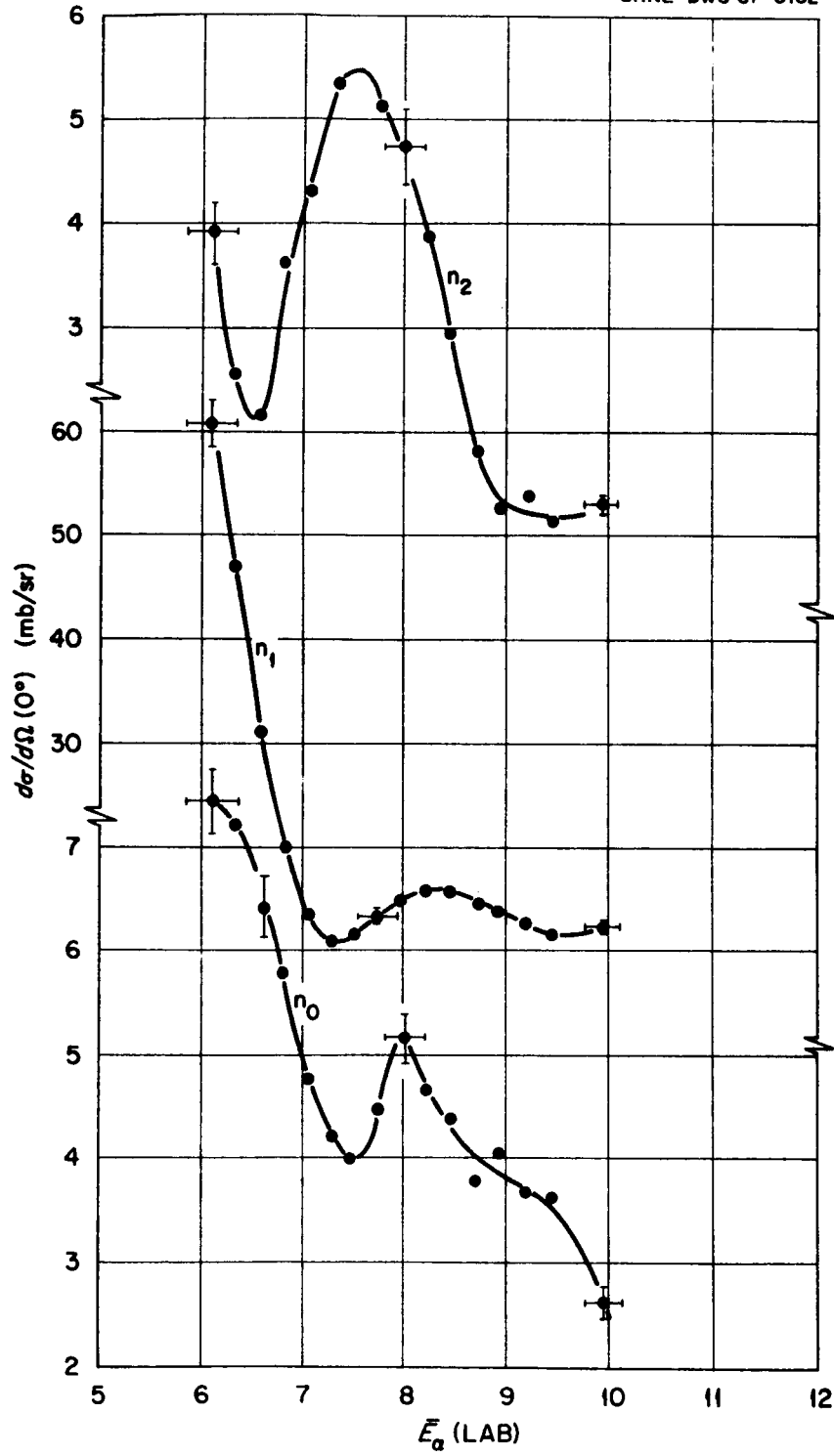
Fig. 6. Excitation Functions for n_0, n_1, n_2 Neutrons at 0 deg (c.m. system) for $\overline{E}_\alpha$ = 6 to 10 MeV.

O-deg cross section for n_1 neutrons) that appeared below the highest n_0 neutron pulses in their data resulted in a substantial loss of accuracy. Our pulse shape discriminator circuit was very effective in rejecting these gamma-ray pulses.

While the O-deg excitation functions are of interest as an independent check on our systematic error, they may be of limited value in showing resonance structure. A slight shift of the forward peak in the neutron angular distribution can result in a very large change of $\sigma(0^\circ)$ without the presence of a corresponding change of $\sigma = \int_\theta \sigma(\theta) \, d\Omega$, the angle-integrated cross section.

IV. THE LOW ENERGY DETAILS OF THE NEUTRON SPECTRA

A. The Energy Spectrum at a Fixed Angle

In Fig. 2, the peaks below the n_2 peak ride on a low-energy continuum which is probably due to the very broad n_4 level under the n_3 peak and some low-energy neutrons from other low-Q-value reactions. Similar structure was observed in careful time-of-flight work at $E_\alpha = 13.5$ and 13.9 MeV and was analyzed by Nilsson and Kjellman.[1] They were able to separate the n_3, n_4, and n_5 levels with the help of shape-analysis of the broad n_4 level. At these values of E_α, the low-energy component from other reactions did not interfere with analysis of the n_3, n_4, and n_5 neutron groups. They found that the n_4 level interfered very slightly with the n_2 level, that it peaked at about the position of the sharper n_3 peak, and that it raised the very weak n_5 peak appreciably. Thus, in Fig. 2, it appears that the n_3 peak is raised mostly by the broad n_4 level. The n_5 peak is raised partly by the tail of the n_4 level, but mostly by low energy neutrons from competing reactions,

such as $^9Be(\alpha,\alpha')^9Be^* \to {}^8Be + n$, $^9Be(\alpha,{}^8Be)^5He \to {}^4He + n$ ($\tau \sim 10^{21}$ sec), and $^9Be(\alpha,n)\,3\alpha$, which have much smaller Q-values than the $^9Be(\alpha,n)^{12}C$ reaction.

B. The Energy Spectrum Integrated over Angle

The neutron production cross section was numerically integrated over angle according to the prescription $\sigma(E_i) = \Sigma_j\,\sigma(\theta_j,E_i)\,\Delta\Omega$. The results for $E_\alpha = 6.79$ and 9.92 MeV are shown in Fig. 7. These spectra show much structure at high neutron energies, as expected, but also show an evaporation-like component that hardens with increasing E_α. The hardening is indicated by the increase in "nuclear temperature" with E_α (see Table II), where the "temperature" was obtained from the slope of a plot of $\sigma(E_n)/\,E_n\sigma_c$ versus E_n (σ_c is the neutron capture cross section of the excited final nucleus, as calculated from continuum theory[13]). This increase in slope implies that the low-energy neutrons must be due to lower Q-value reactions where three- and four-body breakup occurs, such as reactions mentioned in the preceding paragraph, because the level density of ^{12}C is low at these excitation energies. The three-and four-body breakup provides a larger number of degrees of freedom which would explain the presence of the steep slope (and its variation with E_α) at the low energy region of the neutron spectrum.

C. The Total Neutron-Production Cross Section

The integral of each neutron spectrum, such as those shown in Fig. 7, provides the total cross section for the production of neutrons above 0.5 MeV, our spectrometer cutoff. In Table II these totals are compared with the flat-counter results of Gibbons and Macklin[5] who used a 4π graphite integrating sphere to obtain σ(total) as a function of E_α.

ORNL DWG 67-5163
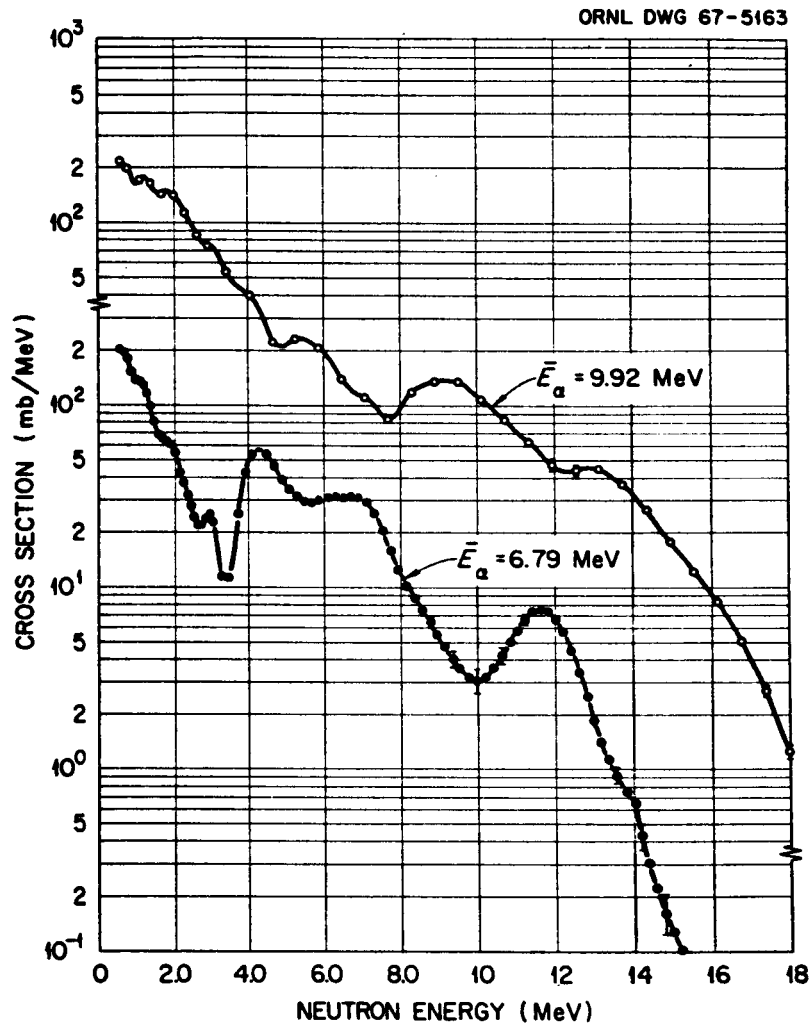

Fig. 7. Angle-Integrated Neutron Cross Sections Versus Neutron Energy (Lab System) for $\bar{E}_\alpha$ = 6.79 and 9.92 MeV.

TABLE II.

Total neutron production cross section as measured with flat counter[5] compared to present results for $E_n > 0.5$ MeV. The hardness of the low energy end of the spectrum is indicated by the reciprocal slope T obtained from a logarithmic plot of $\sigma(E)/\sigma_c E \cong \exp(-E/T)$.

E_α (MeV)	σ_t (mb)	σ_t above 0.5 MeV (mb)	Fraction of total > 0.5 MeV	Reciprocal slope T (MeV)
6.79	570	390	0.69	0.52
7.96	660	466	0.71	0.57
8.91	755	535	0.71	0.68
9.92	703	518	0.74	0.95

Above 0.5 MeV, we obtain about 70% of their total cross section. Our results are in agreement with theirs if we maintain roughly the same slope (see Fig. 7) and integrate the results to zero-MeV neutron energy. The persistence of these steep slopes at very low neutron energies, for all four values of bombarding energy E_α, can also be much more plausibly explained with breakup reactions than with the $^9\text{Be}(\alpha,n)^{12}\text{C}$ reaction. The above inferences assume that there are no systematic differences in absolute normalization of the present results and those of Gibbons and Macklin,[5] a reasonable assumption since both sets of measurements employed the same targets, Faraday cup, current integrator, Van de Graaff accelerator and analyzing magnets.

V. SUMMARY AND CONCLUSIONS

From the present data, and those of Refs. 3 and 4, the angular distribution for the n_0 neutron group is somewhat insensitive to bombarding energy for $E_\alpha \geq 8$ MeV. (This observation is at variance with the conclusion of Deconninck et al.,[14] who have measured $\sigma_0(\theta)$ and $\sigma_1(\theta)$ between 13 and 23 MeV. Although there are similarities between their angular distributions and those of Kondo et al.,[4] for $E_\alpha = 17.5$ to 22 MeV and those of Kjellman and Nilsson[3] for $E_\alpha = 10$ to 14 MeV, it is not clear that there is substantial fluctuation in the n_0 angular distribution between 13 and 17 MeV.) The slow variation of the angular distribution is perhaps due to direct interactions, with very little if any interference from compound nucleus effects. It would therefore be interesting to compare these results with distorted wave Born approximation (DWBA) calculations in which varying proportions of knock-out and heavy-particle stripping are used as fitting parameters. Such fitting has been done for a similar reaction, $^{13}\text{C}(\alpha,n)^{16}\text{O}$, but with a

plane wave Born approximation calculation.[15] The three-peaked angular distribution was fitted well with about equal parts of knock-out and heavy-particle stripping incoherently added. Unfortunately, the plane wave Born approximation is probably too crude an approximation to DWBA calculations (e.g. see Ref. 16) and some backward peaking can be obtained with DWBA calculations without assuming the heavy-particle stripping mechanism of Owen and Madansky.[17]

The neutron spectra at low energies show a strong low-energy component in the forward hemisphere. Integration of these spectra over angle results in a spectrum $\sigma(E)$ with a low energy component that behaves much like that expected for three- and four-body breakup reactions of relatively low Q-value. Integrating this spectrum from the 0.5-MeV spectrometer cutoff to maximum neutron energy, and comparing the results with the total cross section measured with a 4π flat counter,[5] we find that the low-energy component contributes appreciably to the total $^9Be(\alpha,n)$ yield. This finding is of interest in the shielding of space vehicles that may be exposed to solar flare alpha particles,[18] since beryllium alloys are good candidates for construction of the skin material of such vehicles. In fact, this area of interest provided the initial motivation and the support of the present work.

ACKNOWLEDGMENTS

REFERENCES

1. A. Nilsson and J. Kjellman, Nucl. Phys. 32, 177 (1962).

2. N. H. Gale and J. B. Garg, Nuovo Cimento XIX 4, 742 (1961).

3. J. Kjellman and A. Nilsson, Arkiv Fysik 22, 277 (1962).

4. M. Kondo, T. Yamazaki and S. Yamabe, Jour. Phys. Soc. Japan 18, 22 (1963).

5. J. H. Gibbons and R. L. Macklin, Phys. Rev. 114, 571 (1959); 137, B1508 (1965).

6. M. Forté, A. Konsta, and C. Maranzana, "Electronic Methods for Discrimination of Scintillation Shapes," IAEA Conf. on Nuclear Electronics, Belgrade, Paper NE-59 (1961); V. V. Verbinski, W. R. Burrus, R. M. Freestone and R. Textor, "Proton-Recoil Neutron Spectrometry with Organic Scintillators," IAEA Conf. on Neutron Monitoring, Vienna, Paper No. SM-76/13 (1966).

7. W. R. Burrus and V. V. Verbinski, Trans. Amer. Nucl. Soc. 7, 373 (1964); W. R. Burrus and V. V. Verbinski, "Fast Neutron Spectrometry with Thick Organic Scintillators" To be published. W. R. Burrus and J. D. Drischler, The FERDoR Unfolding Code, ORNL 4154 (unpublished).

8. V. V. Verbinski, W. R. Burrus, R. Textor, T. A. Love, and W. Zobel, "Neutron Response of an NE 213 Scintillator from 0.2 to 22 MeV" (to be published). Also V. V. Verbinski et al., Trans. Am. Nucl. Soc. 7, 374 (1964).

9. B. G. Whitmore and W. B. Baker, Phys. Rev. 78, 799 (1950).

10. S. Notarrigo, R. Parisi and A. Rubbino, Nucl. Phys. 29, 509 (1962).

11. E. R. Graves and R. W. Davis, Phys. Rev. 97, 1205 (1955).

12. R. G. Miller and R. W. Kavanagh, Nucl. Phys. $\underline{88}$, 492 (1955).

13. J. M. Blatt and V. F. Weisskopf, Theoretical Nuclear Physics, John Wiley, New York (1952).

14. G. Deconninck, M. de Vroey, J. B. Meulders, and J. Simonet, Nucl. Phys. $\underline{49}$,424 (1963).

15. A. Nilsson and J. Kjellman, Arkiv Fysik $\underline{21}$, 551 (1962).

16. T. B. Day, L. S. Rodberg, and J. Sucher, Phys. Rev. $\underline{123}$, 1051. (1961). W. Tobocman, Phys. Rev. $\underline{115}$, 98 (1959).

17. G. E. Owen and L. Madansky, Phys. Rev. $\underline{105}$, 1766 (1957).

18. P. S. Freier and W. R. Webber, Journal of Geophysical Research $\underline{68}$, 1605 (1963).